

LEVEL X

(P)

DA103044

# A Further Study of the Space and Time Stability of a Narrowband Acoustic Signal in the Ocean: Intermediate Range Results

A Paper Presented at the 101st Meeting of the  
Acoustical Society of America, 20 May 1981,  
Ottawa, Canada

P. E. Herstein  
P. J. Koenigs  
D. G. Browning  
Surface Ship Sonar Department

DTIC  
ELECTED  
AUG 18 1981  
H D



**Naval Underwater Systems Center**  
Newport, Rhode Island / New London, Connecticut

DTIC FILE COPY

Approved for public release; distribution unlimited.

0081818188

### **Preface**

This document was prepared under the Ocean Measurements and Array Technology (OMAT) Program portion of the SEAGUARD Program sponsored by the Defense Advanced Research Projects Agency (ARPA Order No. 2976), Program Manager, V. Simmons, Tactical Technology Office; NUSC Project No. B69605, Program Manager, R. F. LaPlante.

**Reviewed and Approved:**    5 August 1981



**Derek Walters**  
**Surface Ship Sonar Department**

The authors of this document are located at the  
New London Laboratory, Naval Underwater Systems Center,  
New London, Connecticut 06320.

14

## (9) Technical documents.

DD, 1473

7

405918

~~cont'd~~

20. (Continued)

P. D. Koenigs, J. Acoust. Soc. Am. 68(S1), S72(A) 1980). Although the bandwidth remained relatively narrow (approximately 3 mHz), it appeared there were distinct frequency components that could be associated with separate ray groups. In order to verify this, a similar analysis has been conducted at an intermediate range (125 km) where preliminary results indicate the components may be resolvable. Space and time variability are given for percentage Doppler shift, bandwidth and intensity. The results are compared to predictions obtained from the Multipath Expansion Option of the Generic Sonar Model.

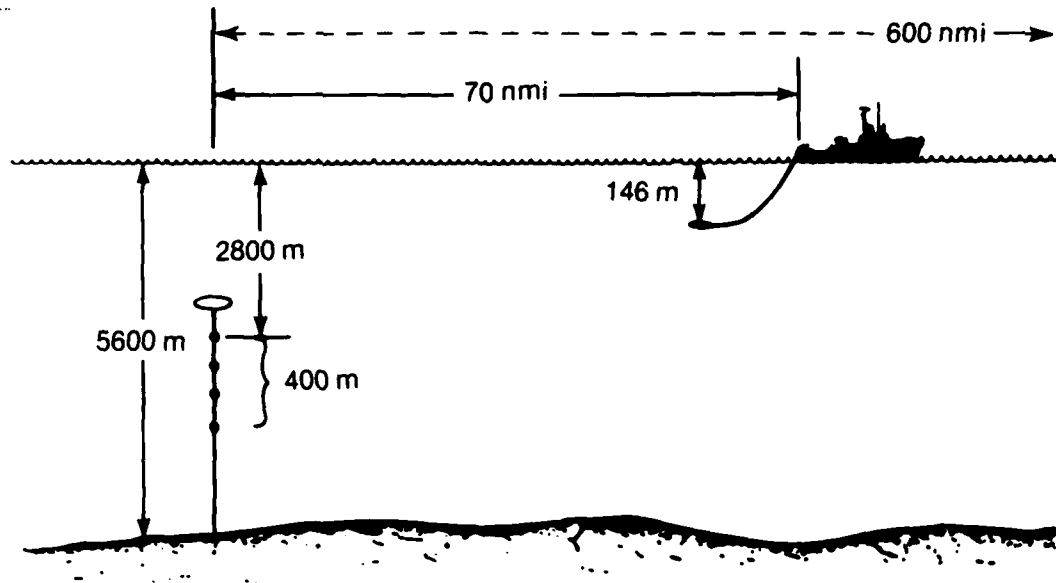
**A Further Study of the Space and Time Stability of a  
Narrowband Acoustic Signal in the Ocean:  
Intermediate Range Results**

**Introduction**

Does the spatial inhomogeneity and temporal instability of the ocean cause narrowband low frequency signals to be transformed into broadband signals? At the last meeting of the Society, we presented the initial analysis of measurements of a narrowband signal when the source-receiver separation was roughly 600 nautical miles. Although the bandwidth remained relatively narrow (roughly 4 millihertz), it appeared there were distinct frequency components that could be associated with separate ray groups. In order to verify this, a similar analysis was conducted at an intermediate range (70 nautical miles) where more distinct ray groups exist. Today, we will present the results of that analysis.

— First slide, please. —

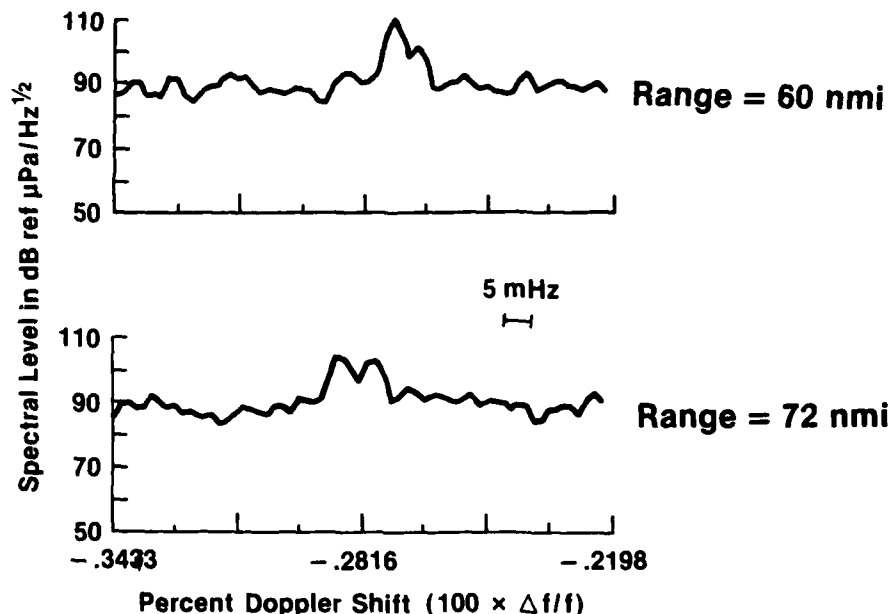
Accession For	
NTIS GRA&I	<input checked="" type="checkbox"/>
DTIC TAB	<input type="checkbox"/>
Unannounced	<input type="checkbox"/>
Justification	
By	
Distribution/	
Availability Codes	
Avail and/or List	Special
PA	

**Viewgraph 1**

Our experiment consisted of towing a very stable low frequency continuous wave (CW) source at an intermediate range interval of 58 to 80 nautical miles, and receiving on four hydrophones vertically spanning 400 meters. The source depth was 146 meters. The vertical array was located near the middle of the water column at a depth of approximately 2800 meters.

— Next slide, please.—

## Representative Received Signal Spectra (H<sub>1</sub>, Avg Time 1074 sec)



**Viewgraph 2**

Shown here are two representative spectra of the received signal on hydrophone 1 (H<sub>1</sub>). The x-axis is percent Doppler shift. The Doppler shift is negative because we are opening range. In the upper spectra, the source receiver separation is nominally 60 nautical miles. Note the dominant peak near the center of the spectra, with a second peak 10 dB lower, roughly 4 millihertz to the right of the dominant peak. In the lower figure, the spectra received at a source/receiver separation of nominally 72 nautical miles is very different. The previously dominant peak has dropped in level so much that there are now two spectral peaks of roughly equal level received through the ocean medium from a CW source.

— Next slide, please. —

## DATA MATRIX

	$T_1$	$T_2$	■	■	■	$T_{23}$	TIME
$H_1$	●	●	●	●	●	●	$\bar{T}_{H_1}$
$H_2$	●	●	●	●	●	●	$\bar{T}_{H_2}$
$H_3$	●	●	●	●	●	●	$\bar{T}_{H_3}$
$H_4$	●	●	●	●	●	●	$\bar{T}_{H_4}$
SPACE AVERAGES	$\bar{S}_{T_1}$	$\bar{S}_{T_2}$				$\bar{S}_{23}$	

### Viewgraph 3

The data are presented in this way: the four hydrophones are designated  $H_1$  through  $H_4$ . Data were processed on each hydrophone for 18 minute periods. This was done 23 times at 9 minute intervals, thus providing a 50% time overlap for each sample. Therefore, we can obtain 23 space average by averaging over the 400 meter vertical extent, and we can also obtain 4 time averages by averaging the data from a single hydrophone over the 23 time intervals. This makes it possible to compare relative changes in time and space for the data sampling. Changes in time are proportional to changes in source/receiver separation for a moving projector.

— Next slide, please. —

## 3 dB Bandwidth Statistics (mHz)

Source/Receiver Separation	Space Average			Time Average		
	Time (min)	$\bar{S}$	$\sigma$	Hydrophone	$\bar{T}$	$\sigma$
Intermediate (70 nmi)	0	4.8	2.9	H1	3.4	1.9
	18	2.7	1.5	H2	3.4	2.0
	36	1.9	0.4	H3	2.9	1.5
	72	3.3	0.9	H4	3.1	1.4
Long (600 nmi)	0	4.0	0.5	H1	3.8	0.6
	18	3.4	0.9	H2	3.6	0.8
	36	3.4	0.6	H3	3.9	0.9
	72	4.2	1.9	H4	3.2	0.3

### Viewgraph 4

Logically, the first parameter to examine is bandwidth. The method was to locate the peak signal in the spectra, and then measure the associated 3 dB bandwidth. Shown here are selected time and space averages and standard deviations of bandwidth measured at both the original 600 nautical mile long range measurements, with 10 samples, and the 70 nautical mile intermediate range results, with 23 samples. These results show that for both space and time the average 3 dB bandwidth of the signal at both the intermediate and long ranges is very narrow, generally, less than 4 millihertz over 9-minute intervals. Note that for the intermediate range results, the standard deviations in both space and time are larger than those at the long range. However, the limitations of this type of standard bandwidth analysis is that the measurement does not include the other lower spectral peaks (as shown in the previous figure) if the other spectral peaks are frequency resolvable.

— Next slide, please. —

## Peak Frequency Statistics

$$\left(\frac{\Delta f}{f}\right) \times 100 \text{ (% Doppler Shift)}$$

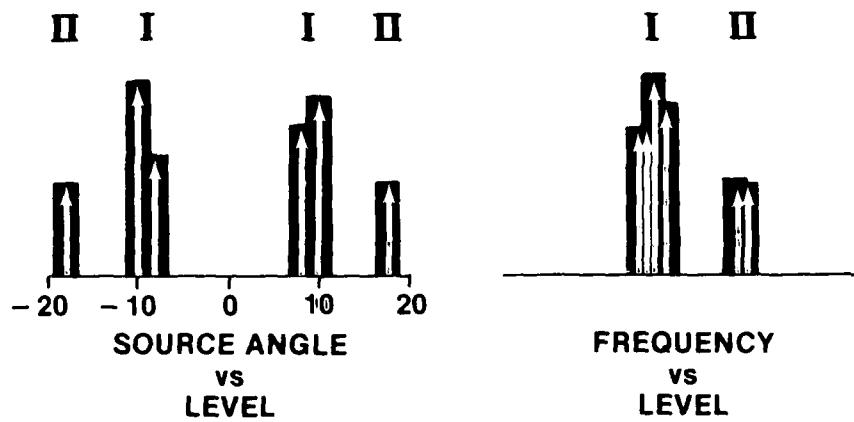
Source/Receiver Separation	Space Average			Time Average		
	Time (min)	$\bar{S}$	$\sigma$	Hydrophone	$\bar{T}$	$\sigma$
Intermediate (70 nmi)	0	.220	.003	H1	.215	.012
	18	.221	.008	H2	.211	.009
	36	.223	.006	H3	.213	.009
	72	.217	.003	H4	.212	.009
Long (600 nmi)	0	.299	.001	H1	.300	.004
	18	.300	.001	H2	.301	.002
	36	.302	.002	H3	.301	.003
	72	.299	.006	H4	.302	.002

### Viewgraph 5

Similarly, the statistics of the peak frequency of the received signal can also be computed, as shown here for both the intermediate and long range results. The mean values for both sets are similar, but the standard deviations are not. For both the space and time measurements, the standard deviations at the intermediate range are greater than the standard deviations at the long ranges. Our long range results were typified by a dominant single peak arrival that was relatively stable. With the multiple peaks observed in the intermediate range results, the peak level "hops" from one peak to a second as a function of depth and range, thus resulting in greater variance in the measurement. Since each peak remains narrow in bandwidth, this greater variance is not representative of bandwidth spreading in the normal "3 dB" sense.

— Next slide, please. —

## EVOLUTION OF SIGNAL BANDWIDTH DUE TO MULTIPATH ARRIVALS AND MOVING SOURCES

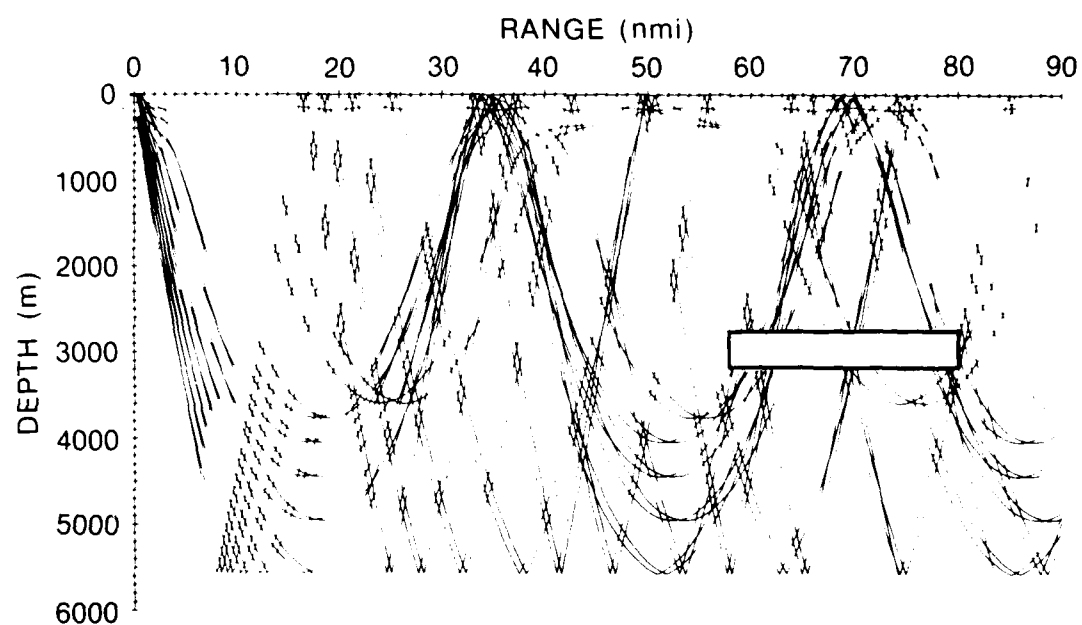


**Viewgraph 6**

What could be the cause for the observed multipath spectra, and how can the observed variability over both range and time be accounted for? Consider the received signal as the multipath summation of individual ray arrivals from the source. Observe the left-hand part of the figure. The arrows show the relative levels of representative raypath arrivals at the receiver for specific source angles. Illustrated are arrivals from two groups. Group I, the relatively shallow angles, are totally refracted paths. Group II, the steeper angles, are bottom reflected paths. Our source is moving so you would expect a Doppler shift that is dependent on the magnitude of the source angle. On the right of the figure are the corresponding Doppler shifts for each of the raypaths shown on the left.

— Next slide, please. —

RAY DIAGRAM  
146 M SOURCE DEPTH  
INCLINATION ANGLES FROM  
- 20 TO + 20 DEG IN 2 DEG STEPS

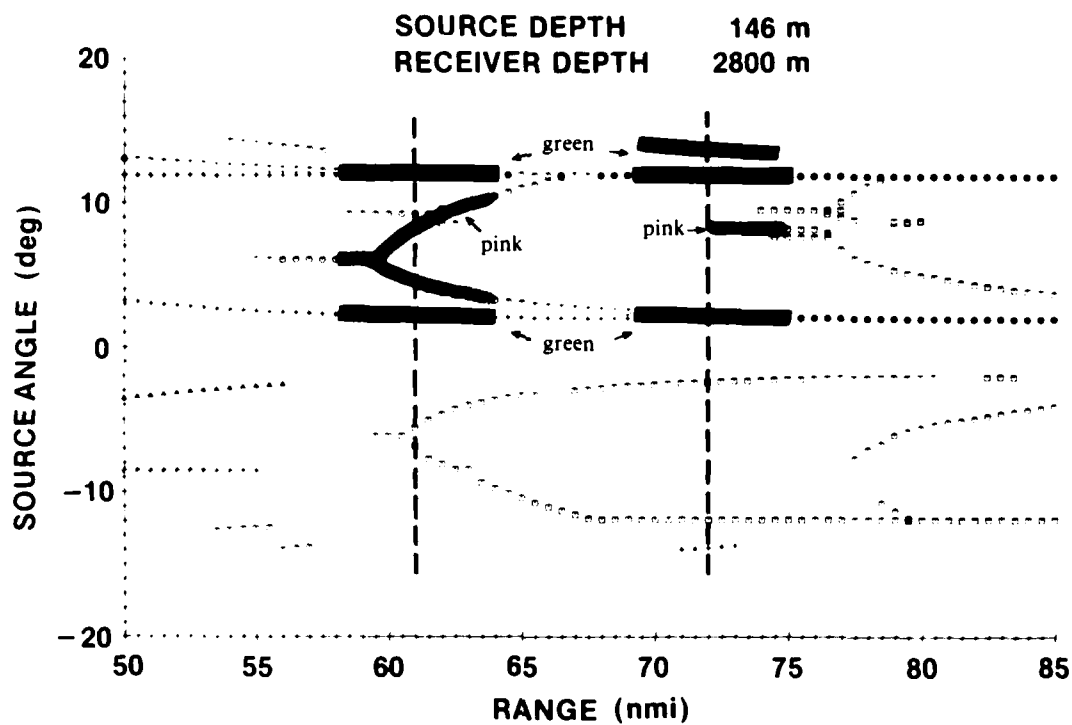


Viewgraph 7

To get an estimate of the possible multipaths that might be present, we used the predictions of the multipath expansion of the generic sonar model developed by Weinberg. This ray plot, with the window at the lower right, shows the region that was covered by this experiment. Since the source is opening range, we are sweeping our 400-meter array across the rays, traveling out to longer ranges.

— Next slide, please. —

## SOURCE ANGLE vs RANGE



**Viewgraph 8**

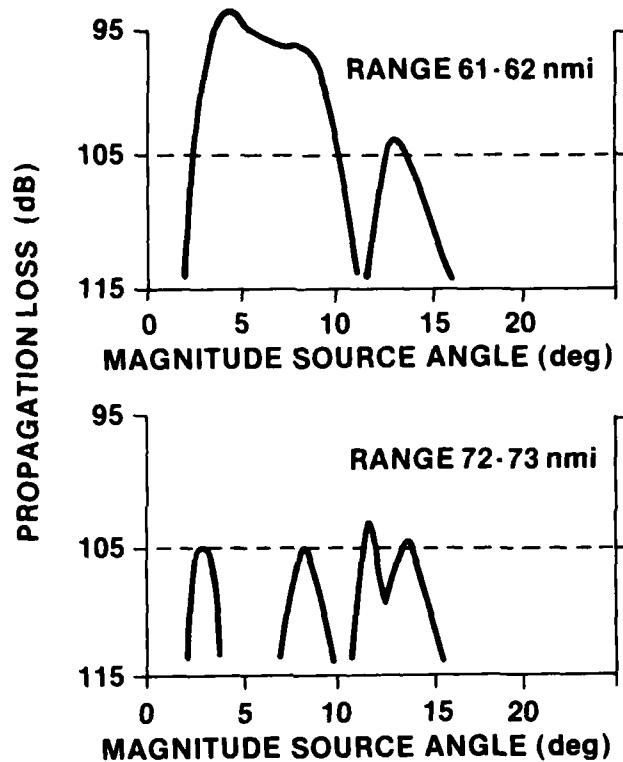
Shown here are the source angles as a function of range for the dominant raypaths for a source at 146 meters and a receiver at 2800 meters. The 'green' raypath source angles near 13 degrees are bottom bounce rays. Note that these rays have source angles that vary only slightly with range. Similarly, the 'green' RSR rays associated with 1 to 3 degrees vary only slightly with range. However, there is another RSR ray group starting at about 59 nautical miles with source angles of  $\pm 6$  degrees. These 'pink' rays, associated with the start of the convergence zone, change rapidly with range, having a characteristic wishbone shape. Note the two dashed lines — at 61 nautical miles (in the convergence zone) and at 72 nautical miles (in-between convergence zones). A significant difference in source angle structure can be clearly seen between the two ranges.

(Viewgraph 8 was originally prepared in color for the presentation.)

— Next slide, please. —

## MODELED PROPAGATION LOSS VS MAGNITUDE OF SOURCE ANGLE

SOURCE DEPTH 146 m  
RECEIVER DEPTH 2800 m

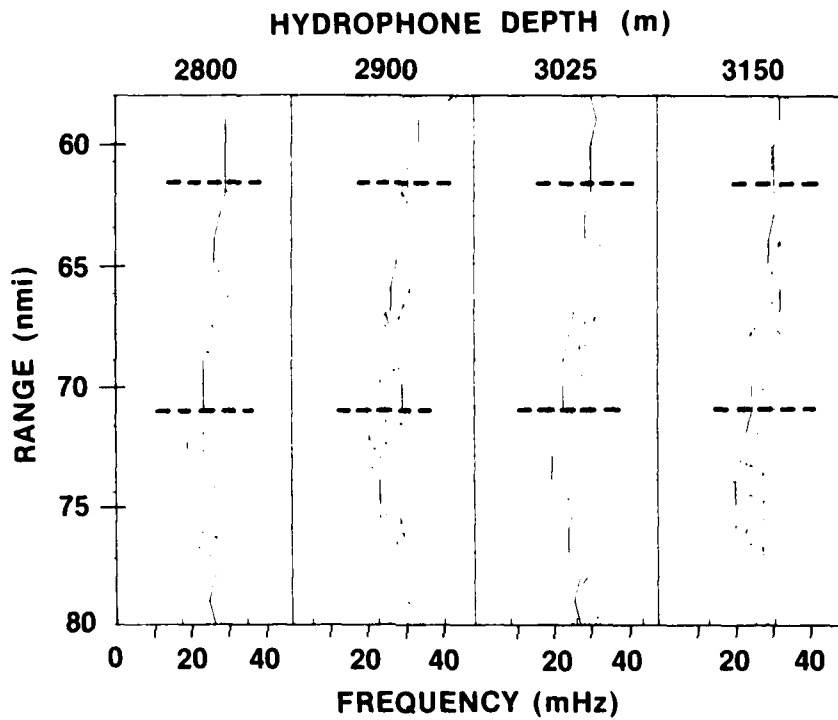


**Viewgraph 9**

Show in the upper figure is the modeled propagation loss as a function of the absolute value of the source angle at 61 nautical miles, while the lower figure shows modeled results at 72 nautical miles. Observe the nearby 10 dB level difference between the peak at 61 nautical miles, in the convergence zone, and the peak at 72 nautical miles, in-between convergence zones. There is a dramatic difference in structure as a function of source angle for the two cases. Recall the transformation relationship between magnitude of the source angle and Doppler shift. Do the measured results show this type of behavior? Yes, as we will now show.

— Next slide, please. —

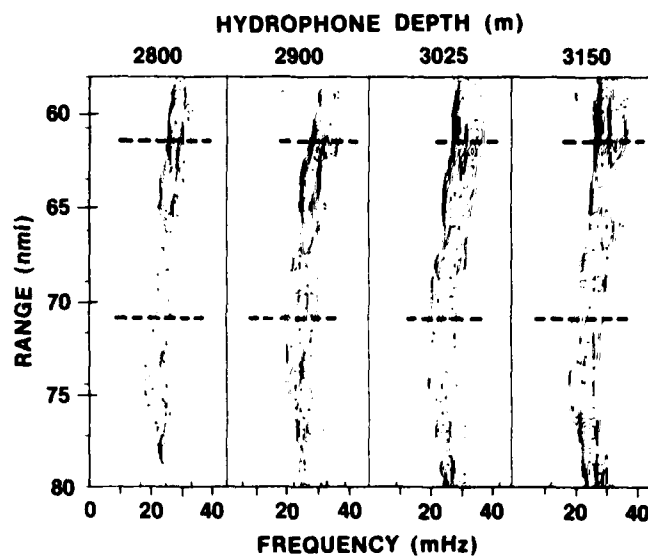
## SIGNAL BANDWIDTH vs RANGE AT FOUR DEPTHS



**Viewgraph 10**

Let's consider measured bandwidth again. Shown here are the 3 and 6 dB standard bandwidth contours as a function of range (y-axis) and frequency (x-axis) for the four hydrophones. The dashed lines mark the ranges at 61 nautical miles and 72 nautical miles, respectively. With the receivers in the convergence zone at 61 nautical miles, relatively uniform narrow bandwidths are observed, characteristic of a single dominant arrival. However, at 72 nautical miles, in-between convergence zones, the results are quite different. Depth dependence is observable. At 2900 and 3025 meters, two distinct peaks can be seen. At 2800 and 3150 meters, considerable bandwidth spreading is also observed.

— Next slide, please. —

**SIGNAL INTENSITY AND DISPERSION VS  
RANGE AT FOUR DEPTHS****Viewgraph 11**

Shown here are contours of signal intensity as a function of range (y-axis) and frequency (x-axis) for the four hydrophones. Contours are in 3 dB intervals decreasing from the maximum peak value. Note again the strong peak in the convergence zone at 61 nautical miles and the frequency dispersion shown by several near equi-level peaks at 72 nautical miles. Also consider the much lower signal intensities at 72 nautical miles as compared with 61 nautical miles.

This presentation has examined the measurement of a low frequency narrowband signal over a source/receiver separation of intermediate range, 58 to 80 nautical miles, with the source, near the surface, moving away from 4 receivers midway in the water column. We can summarize our results as follows:

- As with our previous long range results, isolated single paths remained narrow in bandwidth.
- Variations in received bandwidth and intensity can be directly related to raypath structure.
- Measured received signal levels as a function of Doppler shift correspond to modeled propagation loss as a function of the absolute value of source angle.

At intermediate ranges, therefore, for a moving source narrowband processes will fluctuate considerably in both level and total bandwidth. Both types of fluctuations can be associated with multipath ray structure.

— Slide off, please. —

Thank you, are there any questions?

**Initial Distribution List**

ADDRESSEE	NO. OF COPIES
ARPA Program Office	1
ARPA (R. Fossum, G. Sigman, W. Phillips, CDR V. Simmons, T. Kooij)	5
ARPA Research Center (E. Smith)	1
ASNRE&S (G. Cann)	1
CNM (MAT-08L, D. F. Parrish; MAT 0724, CAPT E. Young)	2
NAVELEX (PME-124: CAPT Cox, CDR D. Jones, CAPT. D. Murton; Code 320)	3
NAVSEASYSCOM (Code 63R, Dr. C. D. Smith; Code 63RA, Dr. R. W. Farwell)	2
NAVPGSCOL (Prof. C. N. K. Mooers; Professor H. Medwin)	2
NORDA (Code 110, Dr. R. R. Goodman; Code 115, R. Martin; Code 521, C. Stuart)	3
NOSC (Code 5313B, Dr. J. R. Lovett)	1
NRL (B. Adams, R. Heitmeyer, W. Moseley, R. Rojas, Dr. A. Berman, Dr. K. M. Guthrie)	6
NUSC Tudor Hill Laboratory (Library)	1
Office of Naval Research (Code 480, Dr. G. R. Hamilton; Code 421, Dr. L. E. Hargrove)	2
SSPO (D. Viccione)	1
U. S. Naval Oceanography Command Center (CDR R. R. Miller)	1
ORI (R. Doolittle, E. Moses)	2
Raytheon Submarine Signal Division (R. Dluhy, R. Pridham, C. Kaufman)	3
MAR, Inc. (J. Franklin, T. Kurpiewski, D. Pelletier, C. Veitch)	4
BBN (J. Heine)	1
Admiralty Underwater Weapons Establishment (D. Stansfield; Dr. D. E. Weston)	2
University of New Hampshire (A. S. Westneat)	1
Computing Devices Co. (K. N. Braun)	1
Marine Physical Laboratory, SCRIPPS (B. Williams, F. H. Fischer)	2
Institute of Geophysics, SCRIPPS (Dr. W. H. Munk)	1
RPI Math Sciences Dept (W. Siegmann)	1
University of Houston (Dr. B. D. Cook)	1
Royal Australian Navy Research Laboratory (Dr. M. Lawrence)	1
Instituto de Pesquisas da Marinha (CDR C. Parente)	1
Yale University (Dr. J. G. Zornig)	1
Case Western Reserve University (Dr. E. B. Yeager)	1
Georgetown University (Dr. W. G. Mayer)	1
University of Tennessee (Dr. M. A. Breazeale)	1
University of Rhode Island (Dr. S. Letcher)	1
ARL, University of Texas (Dr. L. Hampton)	1
University of Bath (Dr. H. O. Berkay)	1
Defence Research Est. Atlantic (Dr. H. M. Merklinger)	1
Defence Research Est. Pacific (Dr. R. Chapman)	1
Technical University of Denmark (Dr. L. Bjorno)	1
Universite Louis Pasteur (Professor S. Candau)	1
Defence Research Centre (Dr. D. H. Brown)	1
SENID (Dr. J. Novarini)	1
DTIC	12